Explicit Nonlinear Model Predictive Control for Autonomous Helicopters

Cunjia Liu, Wen-Hua Chen, John Andrews

Abstract

Trajectory tracking is a basic function required for autonomous helicopters, but it also poses chanlleges to controller design due to the complexity of helicopter dynamics. This paper introduces a closed-form model predictive control (MPC) to solve this problem, which inherents the advantages of the nonlinear MPC but eliminates the time-consuming online optimisation. The explicit solution to the nonlinear MPC problem is derived by using Taylor expansion and exploiting the helicopter model. With the explicit MPC solution, the control signals can be calculated instantaneously to respond to the fast dynamics of helicopters and suppress the disturbances immediately. On the other hand, the online optimisation process can be removed from the MPC framework, which can accelerate the software development and simplify the onboard hardware. Due to these advantages of the proposed method, the overall control framework has a low complexity and high reliability, and it is easy to deploy on the small-scale helicopters. The explicit nonlinear MPC has been successfully validated in simulations and inactual flight tests using the Trex-250 helicopter.

1 Introduction

Autonomous helicopters are increasingly attracting attentions for their potential applications, mainly due to their ability to hover, fly in very low altitudes, and take off and land almost everywhere. These properties make them suitable for a board range of tasks like surveillance, boundary patrol, search and rescue. However, due to their inherent instabilities and nonlinearities and a high dimensional model structure, the controller design for helicopter autonomous flights is a challenge. To this end, a number of control techniques have been applied to address this problem including the classic cascaded PID control [KS03], feedback linearisation [KS98], multivariable adaptive Control [KAM02], neural network adaptive control [JK05], state-dependent riccati equation (SDRE) control [BW07] and composite nonlinear feedback control [PCC$^+$09].

Recently, model predictive control (MPC) has been recognised a promising method in the unmanned aerial vehicle (UAV) community [OM04]. MPC is an optimal control strategy that uses a model to predict the future behaviour of the plant over a prediction horizon. Based on these predictions, the performance index defined to penalise the tracking errors or state errors is minimised with respect to the sequence of

future inputs. Only the first action in the optimised control sequence is applied into the plant, and this procedure is repeatedly executed in a receding horizon fashion to continuously generate control signals. The features of MPC make it as a suitable control technique for UAV applications. Firstly, it naturally takes into account the future value of the reference to improve path tracking performance; secondly, it simplifies the control design by directly using the vehicle model in the control loop; thirdly, it considers both the kinematics and dynamics of UAVs as an entire system in an integrated guidance and control fashion so enhances the flight agility.

The essential procedure in the implementation of MPC algorithm is to solve the formulated optimisation problem (OP). If the system model is linear and there are no constraints acting on the system, the explicit minimisation solution can be found. Otherwise, MPC technique usually requires solving an optimisation problem numerically at every sampling instant, which poses obstacles on the real-time implementation due to the heavy computational burden. Although the development of the avionics and microprocessor technology makes the online optimisation possible, the implementation of computationally demanding MPC on small UAVs is very challenging.

Most of the existing applications tend to use linear MPC so that the formulated OP can be solved by efficient Quadratic Programming [KB06]. To fit the nonlinear tracking problem into a linear setting, associated techniques like linearisation and feedback linearisation techniques are usually required. For nonlinear MPC, although it is more powerful the resulting optimisation problem is non-convex, which means the solving time is much longer and even not deterministic. Therefore, the nonlinear MPC is more likely to be seen in the guidance layer to enhance the autonomy of the UAVs rather than in the time-critical flight control level [HK09]. The associated low bandwidth and computational delay of nonlinear MPC make it very difficult to meet the control requirement for systems with fast dynamics like helicopters. Only few applications on helicopter flight control have been reported in [KSS02, SKS03], where the authors adopt a high-level MPC to solve the tracking problem and rely on a local linear feedback controller to compensate the high-level MPC. Moreover, the formulated nonlinear optimisation problem has to be solved by a secondary flight computer. The extra payload and power consumption are quite luxury for a small-scale helicopter.

To avoid using online optimisation and inherent the advantages of nonlinear MPC, this paper introduces an explicit nonlinear MPC (ENMPC) for trajectory tracking of autonomous helicopters. By approximating the tracking error and control efforts in the receding horizon using their Taylor expansion to a specified order, an analytic solution to nonlinear MPC can be found and consequently the closed form controller can be formulated without online optimisation [CBG03]. The benefits of using this MPC algorithm are not only the elimination of online optimisation and associated resource, but also a higher control bandwidth it can achieve which is very important for helicopters in aggressive flight scenarios. The similar technique has been applied to a glider and a parafoil aircraft, and has shown promising results in the simulations [SKC06]. However, in both the applications, ENMPC was just used to control the vehicle attitude with only inner-loop dynamics under consideration. To

develop a ENMPC for trajectory tracking of autonomous helicopters, the entire helicopter model must be taken into account. A considerable effort is required to develop ENMPC tailored for autonomous trajectory tracking for unmanned helicopters.

To verify the performance of the proposed ENMPC for trajectory tracking of autonomous helicopter, numerical simulations are carried out. The result is also compared with the conventional MPC algorithm when an online optimisation problem is solved at each time instant. Due to the feature of ENMPC, the overall control framework has a low complexity and high reliability, and it is easy to be deployed on the small-scale helicopters. To demonstrate this, flight tests are performed on our indoor testbed using a Trex-250 helicopter.

The remaining part of this paper is organised as follows: Section 2 presents the mathematical model of small-scale helicopters and the simplification for control design; in Section 3 the algorithm of ENMPC and its implementation on autonomous helicopters are discussed in detail; Section 4 provides some simulation and flight experiment results, followed by a conclusion in Section 5.

2 Helicopter modelling

A helicopter is a highly nonlinear system with multiple inputs and multiple outputs and complicated internal couplings. The complete model taking into account the flexibility of the rotors and fuselage usually results in a model of high degrees-of-freedom. The complexity of such a model will make the following system identification much more difficult. However, the general dynamics of a small-scale helicopter can be captured by a six-degrees-of-freedom rigid-body model augmented with a simplified rotor dynamic model [MTK02, GMF01], as shown in Fig.1. Hence, the kinematic relationship of the helicopter, i.e. the position and the orientation represented by Z-Y-X Euler angles, can be expressed as:

$$[\ \dot{x}\quad \dot{y}\quad \dot{z}\ ]^T = \mathbf{R}_b^i(\phi,\theta,\psi)[\ u\quad v\quad w\ ]^T \tag{1}$$

$$\begin{bmatrix}\dot{\phi}\\ \dot{\theta}\\ \dot{\psi}\end{bmatrix} = \begin{bmatrix}1 & \sin\phi\tan\theta & \cos\phi\tan\phi\\ 0 & \cos\phi & -\sin\phi\\ 0 & \sin\phi\sec\theta & \cos\phi\sec\theta\end{bmatrix}\begin{bmatrix}p\\ q\\ r\end{bmatrix} \tag{2}$$

where (x, y, z) describe the helicopter inertial position, (u, v, w) are the local velocities along three body axis, (p, q, r) are angular rates and (ϕ, θ, ψ) are the attitude angles and $\mathbf{R}_b^i$ is a transformation matrix from body to inertial coordinates given in (3) with short notation c for cosine and s for sine.

$$\mathbf{R}_b^i(\phi,\theta,\psi) = \begin{bmatrix} c\theta c\psi & s\phi s\theta c\psi - c\phi s\psi & c\phi s\theta c\psi + s\phi s\psi\\ c\theta s\psi & s\phi s\theta s\psi + c\phi c\psi & c\phi s\theta s\psi - s\phi c\psi\\ -s\theta & s\phi c\theta & c\phi c\theta\end{bmatrix} \tag{3}$$

In terms of the dynamics model, the helicopter is driven by the external forces and moments which are primarily generated by main and tail rotor thrusts, fin and fuselage drags. This means that they are dependent on both the rotor and the rigid-body states. The four control inputs, comprising longitudinal and lateral cyclic pitch,

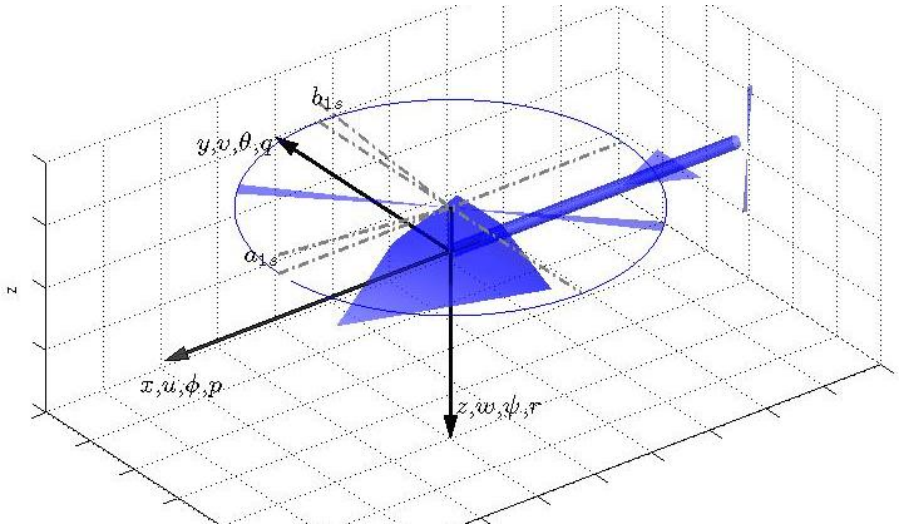

Figure 1: Helicopter frame

main rotor collective pitch and tail collective pitch, alter the states of the main rotor and the trail rotor and consequently exert their influences on the helicopter fuselage. In the control design, the external forces and moments can be approximated by the linear combination of states and control inputs using stability and control derivatives, but the other interactions remain a nonlinear relationship. The model structure is represented in (4).

$$
\begin{aligned}
\dot{u} &= vr - wq - g\sin\theta + X_u u + X_a a \\
\dot{v} &= wp - ur + g\cos\theta\sin\phi + Y_v v + Y_b b \\
\dot{w} &= uq - vp + g\cos\theta\cos\phi + Z_w w + Z_{col}\delta_{col} - g \\
\dot{p} &= L_a a + L_b b \\
\dot{q} &= M_a a + M_b b \\
\dot{r} &= N_r r + N_{col}\delta_{col} + N_{ped}\delta_{ped} \\
\dot{a} &= -q - \frac{a}{\tau} + \frac{A_{lat}}{\tau}\delta_{lat} + \frac{A_{lon}}{\tau}\delta_{lon} \\
\dot{b} &= -p - \frac{b}{\tau} + \frac{B_{lat}}{\tau}\delta_{lat} + \frac{B_{lon}}{\tau}\delta_{lon}
\end{aligned}
\tag{4}
$$

where the dynamics of the main rotor is described by the flapping angles $[\ a \quad b\ ]^T$ with the effective time constant τ; $\mathbf{u} = [\ \delta_{lat} \quad \delta_{lon} \quad \delta_{ped} \quad \delta_{col}\ ]^T$ is the control inputs including lateral and longitudinal cyclic pitch, tail and main rotor collective pitch respectively; the other parameters in the model structure are the stability and control derivatives, whose values are obtained by system identification.

In this model, the rotor flapping states a and b cannot be directly measured, which usually rely on a state observer. In order to reduce the complexity and focus on the control design, we use steady state approximation as a measurement of the

flapping angles [BW07]:

$$\begin{aligned} a &= -\tau q + A_{lat}\delta_{lat} + A_{lon}\delta_{lon} \\ b &= -\tau p + B_{lat}\delta_{lat} + B_{lon}\delta_{lon} \end{aligned} \tag{5}$$

whose values are inserted to the model to replace the state values of a and b, such that

$$\begin{aligned} \dot{p} &= -L_{pq} + L_{lat}\delta_{lat} + L_{lon}\delta_{lon} \\ \dot{q} &= -M_{pq} + M_{lat}\delta_{lat} + M_{lon}\delta_{lon} \end{aligned} \tag{6}$$

where

$$\begin{aligned} L_{pq} &= \tau(L_a q + L_b p), & M_{pq} &= \tau(M_a q + M_b p), \\ L_{lat} &= L_a A_{lat} + L_b B_{lat}, & M_{lat} &= M_a A_{lat} + M_b B_{lat}, \\ L_{lon} &= L_a A_{lon} + L_b B_{lon}, & M_{lon} &= M_a A_{lon} + M_b B_{lon}, \end{aligned} \tag{7}$$

On the other hand, the helicopter suffers slightly unstable zero dynamics introduced by the couplings between the rotor and fuselage [KS98], which are reflected on derivatives X_a and Y_b in (4). Due to the small magnitudes of the flapping angles, these terms can be safely neglected such that the dominate force is the main rotor thrust only. This simplification is quite common in controller design of vertical take-off and landing (VTOL) vehicles [MN07].

The simplified helicopter model by combining (1)-(6) can be expressed in the following compact form:

$$\begin{aligned} \dot{\mathbf{x}} &= f(\mathbf{x}) + g(\mathbf{x})\mathbf{u} \\ \mathbf{y} &= h(\mathbf{x}) \end{aligned} \tag{8}$$

where $\mathbf{x} = [\ x \quad y \quad z \quad u \quad v \quad w \quad p \quad q \quad r \quad \phi \quad \theta \quad \psi\ ]'$ is the helicopter state and $\mathbf{y}$ is the output of the helicopter. In the trajectory tracking control of an autonomous helicopter, the interested outputs are the position and heading angle. Thus, $\mathbf{y} = [\ x \quad y \quad z \quad \psi\ ]^T$.

3 Closed-form MPC

Trajectory tracking is the basic function required when an autonomous helicopters performs a task. To this end, we need design a controller such that the output $\mathbf{y}(t)$ of the helicopter (8) tracks the prescribed reference $\mathbf{w}(t)$. In the MPC strategy, tracking control can be achieved by minimising a receding horizon performance index

$$J = \frac{1}{2}\int_0^T (\hat{\mathbf{y}}(t+\tau) - \mathbf{w}(t+\tau))^T Q(\hat{\mathbf{y}}(t+\tau) - \mathbf{w}(t+\tau))d\tau \tag{9}$$

where weighting matrix $Q = \mathrm{diag}\{q_1, q_2, q_3, q_4\}$, $q_i > 0$, $i = 1, 2, 3, 4$. Note that the hatted variables belong to the prediction time frame.

Conventional MPC algorithm requires solving of an optimisation problem at every sampling instant to obtain the control signals. To avoid the computationally intensive online optimisation, we adopt an explicit solution for the nonlinear MPC problem based on the approximation of the tracking error in the receding prediction horizon.

3.1 Output approximation

For a nonlinear MIMO system like the helicopter, it is well known that after differentiating the outputs for a specific number of times, the control inputs appear. The number of times of differentiation is defined as *relative degree*. For the helicopter with output $\mathbf{y} = [\ x \quad y \quad z \quad \psi\ ]'$ and the corresponding input $\mathbf{u} = [\ \delta_{lon} \quad \delta_{lat} \quad \delta_{col} \quad \delta_{ped}\ ]$, the relative degree is a vector, $\rho = [\ \rho_1 \quad \rho_2 \quad \rho_3 \quad \rho_4\ ]$. If continuously differentiating the output after the control input appears, the derivatives of control input appear, where the number of the input derivatives r is defined as the *control order*.

Since the helicopter model has different relative degrees, the control order r is first specified in the controller design. The ith output of the helicopter in the receding horizon can be approximated by its Taylor series expansion up to order $\rho_i + r$:

$$\begin{aligned}\hat{y}_i(t+\tau) &\approx y_i(t) + \tau\dot{y}_i(t) + \cdots + \frac{\tau^{r+\rho_i}}{(r+\rho_i)!}y_i^{[r+\rho_i]}(t) \\ &= \begin{bmatrix}1 & \tau & \cdots & \frac{\tau^{r+\rho_i}}{(r+\rho_i)!}\end{bmatrix}\begin{bmatrix} y_i(t) \\ \dot{y}_i(t) \\ \cdots \\ y_i^{[r+\rho_i]}(t)\end{bmatrix}\end{aligned} \tag{10}$$

where $i = 1, 2, 3, 4$. In this way, the approximation of the overall output of the helicopter can be cast in a matrix form:

$$\begin{aligned}\hat{\mathbf{y}}(t+\tau) &= \begin{bmatrix}\hat{x}(t+\tau) \\ \hat{y}(t+\tau) \\ \hat{z}(t+\tau) \\ \hat{\psi}(t+\tau)\end{bmatrix} = \begin{bmatrix}\hat{y}_1(t+\tau) \\ \hat{y}_2(t+\tau) \\ \hat{y}_3(t+\tau) \\ \hat{y}_4(t+\tau)\end{bmatrix} \\ &= \begin{bmatrix}1, \tau, \cdots, \frac{\tau^{r+\rho_1}}{(r+\rho_1)!} & \cdots & 0_{1\times(r+\rho_4+1)} \\ \cdots & \cdots & \cdots \\ 0_{1\times(r+\rho_1+1)} & \cdots & 1, \tau, \cdots, \frac{\tau^{r+\rho_4}}{(r+\rho_4)!}\end{bmatrix}\begin{bmatrix} y_1(t) \\ \dot{y}_1(t) \\ \cdots \\ y_1^{[r+\rho_1]}(t) \\ \cdots \\ y_4(t) \\ \dot{y}_4(t) \\ \cdots \\ y_4^{[r+\rho_4]}(t)\end{bmatrix}\end{aligned} \tag{11}$$

For each channel in the output matrix, the control orders r are the same and can be decided during the control design, whereas the relative degrees ρ_i are different but determined by the helicopter model structure. Manipulating the output matrix (11) gives the following partition:

$$\begin{aligned}\hat{\mathbf{y}}(t+\tau) = &\left[\begin{array}{ccc|ccc} \bar{\tau}_1 & \cdots & 0_{1\times\rho_4} & & & \\ \cdots & \cdots & \cdots & \tilde{\tau}_1 & \cdots & \tilde{\tau}_{r+1} \\ 0_{1\times\rho_1} & \cdots & \bar{\tau}_4 & & & \end{array}\right] \\ &\left[\bar{Y}_1(t)^T \quad \cdots \quad \bar{Y}_4(t)^T | \tilde{Y}_1(t)^T \quad \cdots \quad \tilde{Y}_r(t)^T\right]^T\end{aligned} \tag{12}$$

where

$$\bar{Y}_i = \begin{bmatrix} y_i(t) & \dot{y}_i(t) & \cdots & y_i^{[\rho_i-1]} \end{bmatrix}^T, i = 1,2,3,4 \tag{13}$$

$$\tilde{Y}_i = \begin{bmatrix} y_1^{[\rho_1+i-1]} & y_2^{[\rho_2+i-1]} & \cdots & y_4^{[\rho_4+i-1]} \end{bmatrix}^T, i = 1,\ldots,r+1 \tag{14}$$

$$\bar{\tau}_i = \begin{bmatrix} 1 & \tau & \cdots & \frac{\tau^{\rho_i-1}}{(\rho_i-1)!} \end{bmatrix}, i = 1,2,3,4 \tag{15}$$

and

$$\tilde{\tau} = \text{diag}\begin{Bmatrix} \frac{\tau^{\rho_1+i-1}}{(\rho_1+i-1)!} & \cdots & \frac{\tau^{\rho_4+i-1}}{(\rho_4+i-1)!} \end{Bmatrix} \tag{16}$$

It can be observered from Eq(12) that the prediction of the helicopter output $\hat{\mathbf{y}}(t+\tau)$, $0 \le \tau \le T$, in the receding horizon needs the derivatives of each output of the helicopter up to $r+\rho_i$ order at time instant t. Except for the output $\mathbf{y}(t)$ itself that can be directly measured, the other derivatives have to be derived according to the helicopter model (8). During this process the control input will appear in the ρ_ith derivatives, where $i = 1,2,3,4$.

The first derivatives can be obtained from the helicopter's kinematics model:

$$\begin{bmatrix} \dot{y}_1 \\ \dot{y}_2 \\ \dot{y}_3 \end{bmatrix} = \begin{bmatrix} \dot{x} \\ \dot{y} \\ \dot{z} \end{bmatrix} = \mathbf{R}_b^i \cdot \begin{bmatrix} u \\ v \\ w \end{bmatrix} \tag{17}$$

$$\dot{y}_4 = \dot{\psi} = q\sin\phi\sec\theta + r\cos\phi\sec\theta \tag{18}$$

Differentiating (17) and (18) with substitution of helicopter dynamics (4) yields the second derivatives:

$$\begin{bmatrix} \ddot{y}_1 \\ \ddot{y}_2 \\ \ddot{y}_3 \end{bmatrix} = \begin{bmatrix} \ddot{x} \\ \ddot{y} \\ \ddot{z} \end{bmatrix} = \mathbf{R}_b^i \begin{bmatrix} 0 \\ 0 \\ T \end{bmatrix} + \begin{bmatrix} 0 \\ 0 \\ g \end{bmatrix}, \tag{19}$$

where $T = Z_w w + Z_{col}\delta_{col} - g$ is the nomarlised main rotor thrust (intermedia steps given in apendix A), and

$$\begin{aligned} \ddot{y}_4 = \ddot{\psi} = {} & q\frac{\cos\phi}{\cos\theta}\dot{\phi} + q\frac{\sin\phi\sin\theta}{\cos^2\theta}\dot{\theta} - r\frac{\sin\phi}{\cos\theta}\dot{\phi} + r\frac{\cos\phi\sin\theta}{\cos^2\theta}\dot{\theta} - \\ & L_{pq}\frac{\sin\phi}{\cos\theta} + N_r\frac{\cos\phi}{\cos\theta} + \begin{bmatrix} L_{lat}\frac{\sin\phi}{\cos\theta} & L_{lon}\frac{\sin\phi}{\cos\theta} & N_{col}\frac{\cos\phi}{\cos\theta} & N_{ped}\frac{\cos\phi}{\cos\theta} \end{bmatrix}\mathbf{u} \end{aligned} \tag{20}$$

where $\mathbf{u}$ is the control vector. Note that although control input δ_{col} appears in (19), the other control inputs do not, so we have to continue differentiating the first three outputs. To facilitate the derivation, we adopt the relationship $\dot{\mathbf{R}}_b^i = \mathbf{R}_b^i\hat{\omega}$ by using skew-symmetric matrix $\hat{\omega} \in \mathbb{R}^{3\times3}$:

$$\hat{\omega} = \begin{bmatrix} 0 & -r & q \\ r & 0 & -p \\ -q & p & 0 \end{bmatrix}. \tag{21}$$

Thus, the third and fourth derivatives of the position output can be written in:

$$\begin{bmatrix} y_1^{[3]} \\ y_2^{[3]} \\ y_3^{[3]} \end{bmatrix} = \begin{bmatrix} x^{[3]} \\ y^{[3]} \\ z^{[3]} \end{bmatrix} = \mathbf{R}_b^i\hat{\omega}\begin{bmatrix} 0 \\ 0 \\ T \end{bmatrix} + \mathbf{R}_b^i\begin{bmatrix} 0 \\ 0 \\ Z_w\dot{w} + Z_{col}\dot{\delta}_{col} \end{bmatrix}, \tag{22}$$

and

$$\begin{bmatrix} y_1^{[4]} \\ y_2^{[4]} \\ y_3^{[4]} \end{bmatrix} = \begin{bmatrix} x^{[4]} \\ y^{[4]} \\ z^{[4]} \end{bmatrix} = \mathbf{R}_b^i \hat{\omega}\hat{\omega} \begin{bmatrix} 0 \\ 0 \\ T \end{bmatrix} + 2\mathbf{R}_b^i \hat{\omega} \begin{bmatrix} 0 \\ 0 \\ Z_w \dot{w} + Z_{col}\dot{\delta}_{col} \end{bmatrix} + \mathbf{R}_b^i \begin{bmatrix} -M_{pq}T \\ L_{pq}T \\ Z_w \ddot{w} \end{bmatrix} + \mathbf{R}_b^i \begin{bmatrix} M_{lat}T & M_{lon}T & 0 \\ -L_{lat}T & -L_{lon}T & 0 \\ 0 & 0 & Z_{col} \end{bmatrix} \begin{bmatrix} \delta_{lat} \\ \delta_{lon} \\ \ddot{\delta}_{col} \end{bmatrix} \quad (23)$$

At this stage, the control inputs explicitly appear in (23). Therefore, the vector relative degree for the helicopter is $\rho = [\ 4 \quad 4 \quad 4 \quad 2\ ]$. Note that in the formulation of (23) $\ddot{\delta}_{col}$ is the new control input, whereas δ_{col} and $\dot{\delta_{col}}$ are treated as the states which can be obtained by adding integrators.

By invoking (17) -(22), we now can construct matrix $\bar{Y}_i$, $i = 1, 2, 3, 4$. However, in order to find the elements in $\tilde{Y}_i$, $i = 1, 2, \ldots, r+1$, further manipulation is required. By combining (20) and (23) and utilizing the Lie notation [Isi95], we have:

$$\tilde{Y}_1 = \begin{bmatrix} y_1^{[\rho_1]} \\ y_2^{[\rho_2]} \\ y_3^{[\rho_3]} \\ y_4^{[\rho_4]} \end{bmatrix} = \begin{bmatrix} x^{[4]} \\ y^{[4]} \\ z^{[4]} \\ \psi^{[2]} \end{bmatrix} = \begin{bmatrix} L_f^{\rho_1} h_1(\mathbf{x}) \\ L_f^{\rho_2} h_2(\mathbf{x}) \\ L_f^{\rho_3} h_3(\mathbf{x}) \\ L_f^{\rho_4} h_4(\mathbf{x}) \end{bmatrix} + A(\mathbf{x})\tilde{\mathbf{u}} \quad (24)$$

where $\tilde{\mathbf{u}} = [\ \delta_{lat} \quad \delta_{lon} \quad \ddot{\delta}_{col} \quad \delta_{ped}\ ]$; nonlinear terms $L_f^{\rho_i} h_i(\mathbf{x})$, $i = 1, 2, 3, 4$, can be found in the previous derivation, and

$$A(\mathbf{x}) = \left[\begin{array}{ccc:ccc} L_{g_1} L_f^{\rho_1 - 1} h_1(\mathbf{x}) & \cdots & & L_{g_4} L_f^{\rho_1 - 1} h_1(\mathbf{x}) \\ L_{g_1} L_f^{\rho_1 - 1} h_2(\mathbf{x}) & \cdots & & L_{g_4} L_f^{\rho_1 - 1} h_2(\mathbf{x}) \\ \cdots & \cdots & & \cdots \\ \hdashline L_{g_1} L_f^{\rho_1 - 1} h_4(\mathbf{x}) & \cdots & & L_{g_4} L_f^{\rho_1 - 1} h_4(\mathbf{x}) \end{array}\right] = \begin{bmatrix} A_{11} & A_{12} \\ A_{21} & A_{22} \end{bmatrix}. \quad (25)$$

where

$$\begin{aligned} A_{11} &= \mathbf{R}_b^i \begin{bmatrix} M_{lat}T & M_{lon}T & 0 \\ -L_{lat}T & -L_{lon}T & 0 \\ 0 & 0 & Z_{col} \end{bmatrix}, A_{12} = 0_{3\times 1}, \\ A_{21} &= \begin{bmatrix} L_{lat}\frac{\sin\phi}{\cos\theta} & L_{lon}\frac{\sin\phi}{\cos\theta} & 0 \end{bmatrix}, A_{22} = N_{ped}\frac{\cos\phi}{\cos\theta}. \end{aligned} \quad (26)$$

Differentiating (24) with respect to time together with substituation of the system's dynamics gives

$$\tilde{Y}_2 = \begin{bmatrix} y_1^{[\rho_1+1]} \\ y_2^{[\rho_2+1]} \\ y_3^{[\rho_3+1]} \\ y_4^{[\rho_4+1]} \end{bmatrix} = \begin{bmatrix} L_f^{\rho_1+1} h_1(\mathbf{x}) \\ L_f^{\rho_2+1} h_2(\mathbf{x}) \\ L_f^{\rho_3+1} h_3(\mathbf{x}) \\ L_f^{\rho_4+1} h_4(\mathbf{x}) \end{bmatrix} + A(\mathbf{x})\tilde{\mathbf{u}}^{[1]} + p_1(\mathbf{x}, \tilde{\mathbf{u}}) \quad (27)$$

where $p_1(\mathbf{x}, \tilde{\mathbf{u}})$ is a nonlinear vector function of $\mathbf{x}$ and $\tilde{\mathbf{u}}$. By repeating this procedure, the higher derivatives of the output and $\tilde{Y}_i$, $i = 1, 2, \ldots, r$, can be calculated and finally we have

$$\tilde{Y}_{r+1} = \begin{bmatrix} y_1^{[\rho_1+r]} \\ y_2^{[\rho_2+r]} \\ y_3^{[\rho_3+r]} \\ y_4^{[\rho_4+r]} \end{bmatrix} = \begin{bmatrix} L_f^{\rho_1+r} h_1(\mathbf{x}) \\ L_f^{\rho_2+r} h_2(\mathbf{x}) \\ L_f^{\rho_3+r} h_3(\mathbf{x}) \\ L_f^{\rho_4+r} h_4(\mathbf{x}) \end{bmatrix} + A(\mathbf{x})\tilde{\mathbf{u}}^{[r]} + p_r(\mathbf{x}, \tilde{\mathbf{u}}, \tilde{\mathbf{u}}^{[1]}, \ldots, \tilde{\mathbf{u}}^{[r]}) \tag{28}$$

So far by exploiting the helicopter model the elements to construct $\bar{Y}$ and $\tilde{Y}$ are available. Therefore, the output of the helicopter in the future horizon $\mathbf{y}(t+\tau)$ can be expressed by its Taylor expansion in a generalized linear form with respect to the prediction time τ and current states as shown in Eq.(12).

In the same fashion as in Eq.(12), the reference in the receding horizon $w(t+\tau)$ can also be approximated by:

$$\mathbf{w}(t+\tau) = \begin{bmatrix} w_1(t+\tau) \\ w_2(t+\tau) \\ w_3(t+\tau) \\ w_4(t+\tau) \end{bmatrix} = \begin{bmatrix} T_f & T_s \end{bmatrix} \begin{bmatrix} \bar{W}_1(t)^T & \cdots & \bar{W}_4(t)^T | \tilde{W}_1(t)^T & \cdots & \tilde{W}_{r+1}(t)^T \end{bmatrix}^T \tag{29}$$

where

$$T_f = \begin{bmatrix} \bar{\tau}_1 & \cdots & 0_{1\times\rho_4} \\ \vdots & \ddots & \vdots \\ 0_{1\times\rho_1} & \cdots & \bar{\tau}_4 \end{bmatrix} \tag{30}$$

and

$$T_s = \begin{bmatrix} \tilde{\tau}_1 & \cdots & \tilde{\tau}_{r+1} \end{bmatrix} \tag{31}$$

and the construction of $\bar{W}_i(t)$, $i = 1, 2, 3, 4$, and $\tilde{W}_i$, $i = 1, \ldots, r+1$, can refer to the structure of $\bar{Y}_i(t)$ and $\tilde{Y}_i$, respectively.

3.2 Explicit nonlinear MPC solution

The conventional MPC needs to solve a formulated optimisation problem to generate the control signal, where the control performance index is minimised with respect to the future control input over the prediction horizon. In this paper, after the output is approximated by its Taylor expansion, the control profile can be defined as

$$\tilde{\mathbf{u}}(t+\tau) = \tilde{\mathbf{u}}(t) + \tau\tilde{\mathbf{u}}^{[1]}(t) + \cdots + \frac{\tau^r}{r!}\tilde{\mathbf{u}}^{[r]}(t), 0 \le \tau \le T \tag{32}$$

Thereby, the helicopter outputs depend on the control variables $\bar{\mathbf{u}} = \{\ \tilde{\mathbf{u}}, \tilde{\mathbf{u}}^{[1]}, \ldots, \tilde{\mathbf{u}}^{[r]}\ \}$.

Recalling the performance index (9) and the output and reference approximation (12) and (29), we have:

$$J = \frac{1}{2}(\bar{Y}(t) - \bar{W}(t))^T \begin{bmatrix} \mathcal{T}_1 & \mathcal{T}_2 \\ \mathcal{T}_2^T & \mathcal{T}_3 \end{bmatrix} (\bar{Y}(t) - \bar{W}(t)) \tag{33}$$

where

$$\bar{Y}(t) = \begin{bmatrix} \bar{Y}_1(t)^T & \cdots & \bar{Y}_4(t)^T | \tilde{Y}_1(t)^T & \cdots & \tilde{Y}_r(t)^T \end{bmatrix}^T, \tag{34}$$

$$\bar{W}(t) = \begin{bmatrix} \bar{W}_1(t)^T & \cdots & \bar{W}_4(t)^T | \tilde{W}_1(t)^T & \cdots & \tilde{W}_{r+1}(t)^T \end{bmatrix}^T, \tag{35}$$

$$\mathcal{T}_1 = \int_0^T T_f^T Q T_f d\tau, \tag{36}$$

$$\mathcal{T}_2 = \int_0^T T_f^T Q T_s d\tau, \tag{37}$$

and

$$\mathcal{T}_3 = \int_0^T T_s^T Q T_s d\tau. \tag{38}$$

Therefore, instead of minimising the performance index (9) with respect to control profile $\mathbf{u}(t+\tau)$, $0 < \tau < T$ directly, we can minimise the approximated index (33) with respect to $\bar{\mathbf{u}}$, where the necessary condition for the optimality is given by

$$\frac{\partial J}{\partial \bar{\mathbf{u}}} = 0 \tag{39}$$

After solving the nonlinear equation (39), we can obtain the optimal control variables $\bar{\mathbf{u}}^*$ to construct the optimal control profile defined by Eq.(32). As in MPC only the current control in the control profile is implemented, the explicit solution is $\tilde{\mathbf{u}}^* = \tilde{\mathbf{u}}(t+\tau)$, for $\tau = 0$. The resulting controller is given by

$$\tilde{\mathbf{u}}^* = -A(\mathbf{x})^{-1}(KM_\rho + M_1) \tag{40}$$

where $K \in \mathbb{R}^{4\times(\rho_1+\cdots+\rho_4)}$ is the first 4 row of the matrix $\mathcal{T}_3^{-1}\mathcal{T}_2^T \in \mathbb{R}^{4(r+1)\times(\rho_1+\cdots+\rho_4)}$ where the ijth block of $\mathcal{T}_2$ is of $\rho_i \times 4$ matrix, and all its elements are zeros except the ith column is given by

$$\begin{bmatrix} q_i \frac{T^{\rho_i+j}}{(\rho_i+j-1)!(\rho_i+j)} & \cdots & q_i \frac{T^{2\rho_i+j-1}}{(\rho_i+j-1)!(\rho_i-1)!(2\rho_i+j-1)} \end{bmatrix}^T \tag{41}$$

for $i = 1, 2, 3, 4$ and $j = 1, 2, \ldots, r+1$, and ijth block of $\mathcal{T}_3$ is given by

$$\operatorname{diag}\left\{ q_1 \frac{T^{2\rho_1+i+j-1}}{(\rho_1+i-1)!(\rho_1+j-1)!(2\rho_1+i+j-1)}, \cdots, q_4 \frac{T^{2\rho_4+i+j-1}}{(\rho_4+i-1)!(\rho_4+j-1)!(2\rho_4+i+j-1)} \right\} \tag{42}$$

for $i, j = 1, 2, \ldots, r+1$; the matrix $M_\rho \in \mathbb{R}^{\rho_1+\cdots+\rho_4}$ and matrix $M_i \in \mathbb{R}^4$ are defined as:

$$M_\rho = \begin{bmatrix} \bar{Y}_1(t)^T \\ \vdots \\ \bar{Y}_4(t)^T \end{bmatrix} - \begin{bmatrix} \bar{W}_1(t)^T \\ \vdots \\ \bar{W}_4(t)^T \end{bmatrix} \tag{43}$$

and

$$M_i = \begin{bmatrix} L_f^{\rho_1+i-1} h_1(t) \\ L_f^{\rho_2+i-1} h_2(t) \\ \vdots \\ L_f^{\rho_4+i-1} h_4(t) \end{bmatrix} - \tilde{W}_i(t)^T, i = 1, 2, \ldots, r+1. \tag{44}$$

The detailed derivation is provided in the appendix. The overall controller structure is shown in Fig.2.

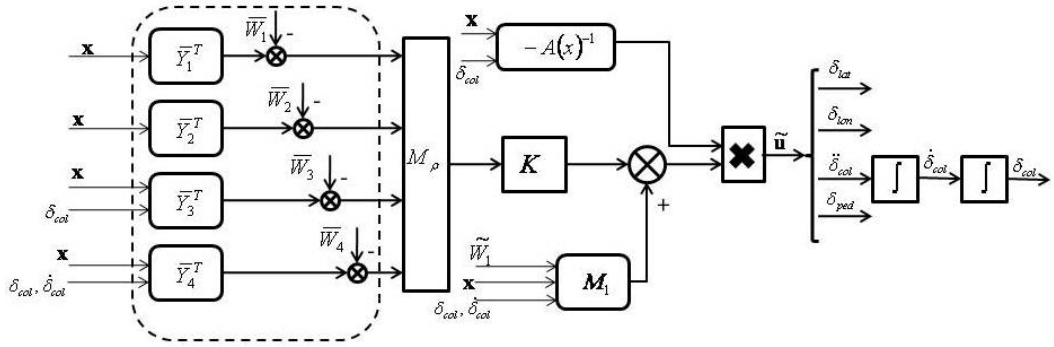

Figure 2: ENMPC structure

3.3 Implementation issue

When the ENMPC is applied for trajectory tracking of autonomous helicopters, not only the reference trajectory is required, the higher derivatives of the reference trajectory with respect to time are also needed in the prediction. Although this can be achieved by using various modern path planning algorithms, there are still some applications where the dedicated path generator is not available. In these cases the reference is more likely to be designed comprising only the demanded helicopter position and the associated heading angle. To address this problem, we adopt a simple but effective method of low-pass prefilter (45), as shown in Fig. 3.

$$G(s) = \frac{\omega_n^2}{s^2 + 2\zeta\omega_n s + \omega_n^2} \tag{45}$$

Given the appropriate parameters ζ and ω, the command prefilter can provide first and second derivatives of the original reference, which is adequate for a smooth trajectory tracking.

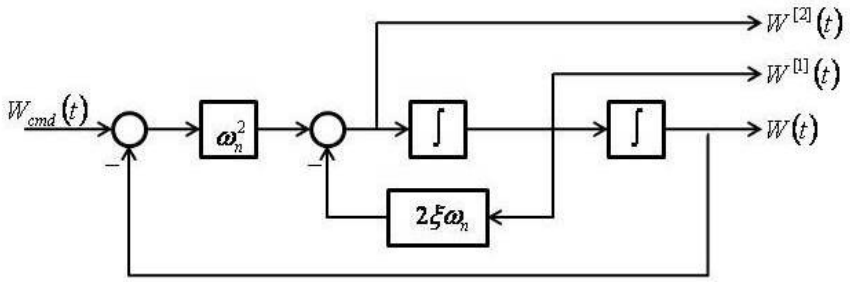

Figure 3: Command prefilter

4 Simulation and experiment

4.1 Simulation

The proposed ENMPC has been validated in simulations and flight experiments. The simulation and experiment are based on the Trex-250 miniature helicopter that is a radio controlled helicopter with a main rotor diameter of 460mm and a trail rotor diameter of 108mm. Trex-250 has a collective pitch rotor and well designed Bell-Hiller stabilizer mechanism which is consistent with most of the small-scale helicopters mentioned in the literature. Moreover, the miniaturized size and aerobatic ability make it well-suited for indoor flight test. The model parameters of Trex-250 have been obtained by comprehensive system identification in the previous work.

Numerical simulations were carried out first to investigate the attained performance of ENMPC and compare it with the conventional MPC supported by the online optimisation [LCA10]. In the simulation, the full dynamic model with 20% parameter uncertainties was used as the plant, whereas the simplified model was just for control synthesis purposes. The ENMPC is designed with the prediction horizon $T = 4s$, control order $r = 4$ and $Q = \text{diag}\{1 \quad 1 \quad 1 \quad 1\}$. The command prefilter parameters are chosen as: $\zeta = 0.7$ and $\omega_b = 10\text{rad/s}$. In the conventional MPC, the prediction horizon is set to $T = 1s$ and the weighting matrix is chosen as the same as in ENMPC, but to penalise the control effort, the control input weighting term $\mathbf{u}^T R\mathbf{u}$ is added into the performance index, where $R = \text{diag}\{0.5 \quad 0.5 \quad 0.5 \quad 0.5\}$. The corresponding optimisation problem is solved by using Matlab function *fmincon*.

In the simulation, the helicopter was required to track a mulit-section reference connected by abrupt turns. The helicopter tracking performance is given in Fig.4. It can be seen that the helicopter under both conventional MPC and ENMPC is able to track the reference with very satisfactory performance. However, in the conventional MPC the average time for solving the formulated OP is about 0.2s, which restricts the control bandwidth to 5Hz. The ENMPC tackles this problem by directly using the explicit solution and can easily reach the required control bandwidth. On the other hand, during the abrupt reference changes, the conventional MPC can replan the local trajectory to adapt to the helicopter dynamics, whereas the ENMPC relying on the command prefilter can also deliver a smooth tracking performance.

4.2 Flight experiment

The proposed ENMPC was further validated through flight experiments which took place on our indoor testbed. Consisting of Trex-250 helicopters, Vicon motion capture system and ground station computers, the testbed combines commercial-off-the-shelf equipments effectively and integrates them into the Matlab environment (see Fig.5). By developing dedicated interfaces, researcher can implement algorithms in Simulink to operate the real helicopter as normal as in the simulation. Thus, the testbed provides a seamless way from the control analysis and design to the experimental validation [LCCAed].

The first flight test is to track a square trajectory with the heading angle fixed

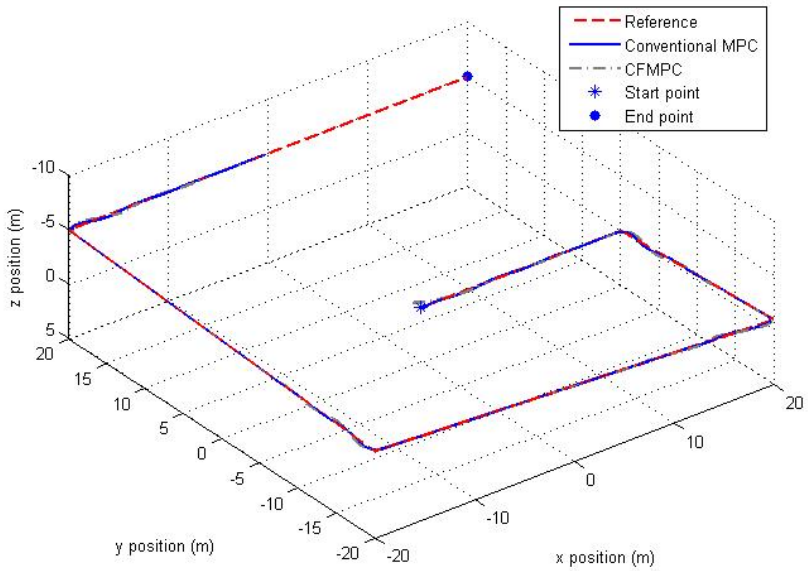

Figure 4: Trajectory tracking results

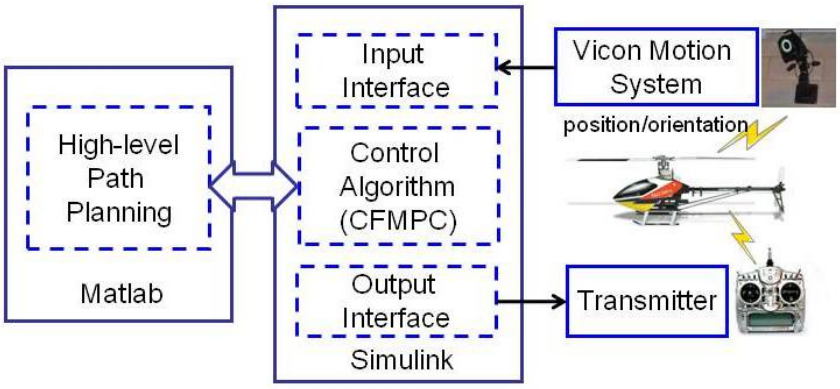

Figure 5: Structure of indoor testbed

at zero. During this process the helicopter exhibits its manoeuvrability along four directions respectively. The tracking result is shown in Fig.6 in a 3-dimensional view with the attitude indicated along the trajectory. With the predictive feature, the helicopter under the control of ENMPC has the smooth and stable tracking capability even if it comes across an abrupt turn. The roll and pitch angle history provided in Fig.7 shows how the lateral and longitudinal channels are coordinated by the controller. During the turning points, the roll angle and pitch angle change together to increase the translational speed at one direction and decrease at another. The corresponding control signals are also given in Fig.8.

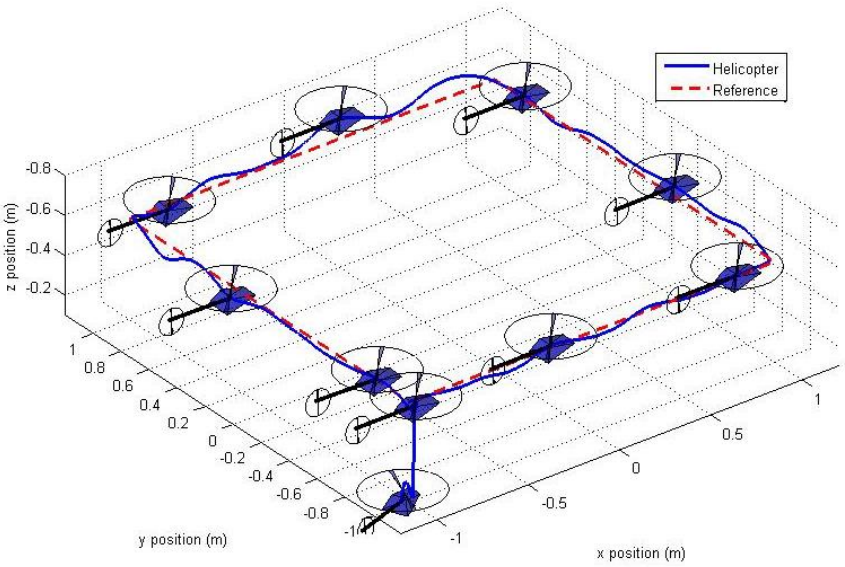

Figure 6: Square trajectory tracking

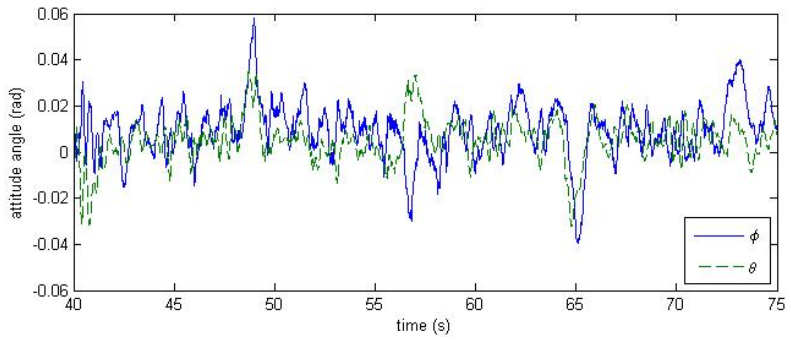

Figure 7: Attitude angles for square tracking

Another flight test was carried out to track a eight-shape trajectory. This flight test is used to show the coordinated heading and position tracking capability that is

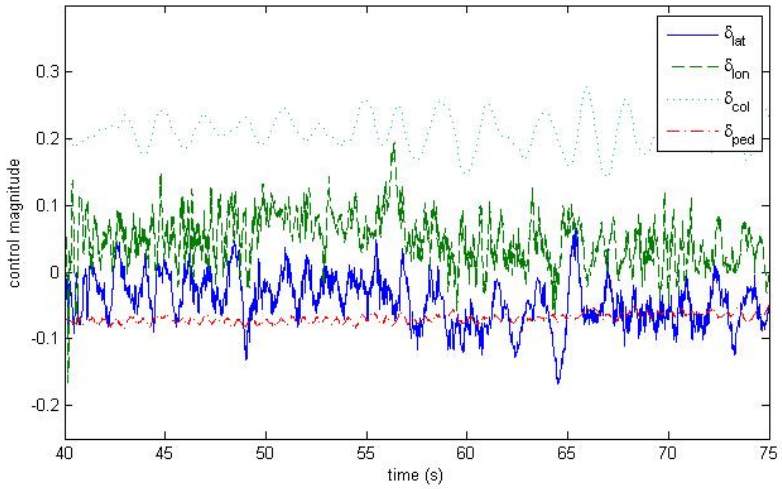

Figure 8: Control signals for square tracking

not demonstrated in the first flight test. Along the reference trajectory the required heading angle w_4 is defined by

$$w_4(t) = \arctan 2(\dot{w}_1(t), \dot{w}_2(t)) \tag{46}$$

where $\arctan 2$ is the four-quadrant inverse tangent function, $\dot{w}_1$ and $\dot{w}_2$ are the reference velocity in x and y directions, respectively. The helicopter tracking result is given in Fig.9 in a 2-dimensional view with heading angle indicated. The control signals are given in Fig.10.

5 Summary

Designing an MPC based controller with "foresee" feature to support the trajectory tracking of autonomous helicopters is a promising but challenging work, as the helicopter is unstable, highly nonlinear and particularly exhibits fast dynamics. To inherent the advantages of the MPC technique and prevent time consuming online optimisation, we introduce a closed-form MPC for the helicopter tracking problem. The explicit solution to the MPC problem is derived by using Taylor expansion and exploiting the helicopter model. With the explicit MPC solution, on one hand the control signals can be calculated instantaneously to respond to the fast dynamics of helicopters and suppress the disturbances immediately. On the other hand, the online optimisation process can be removed from the MPC framework, which can accelerate the software development and simplify the onboard hardware. Due to these advantages of ENMPC, the overall control framework has a low complexity and high reliability, and it is easy to deploy on the small-scale helicopters.

The proposed ENMPC has been successfully validated in simulations and actual flight tests using the Trex-250 helicopter. ENMPC shows a competitive performance

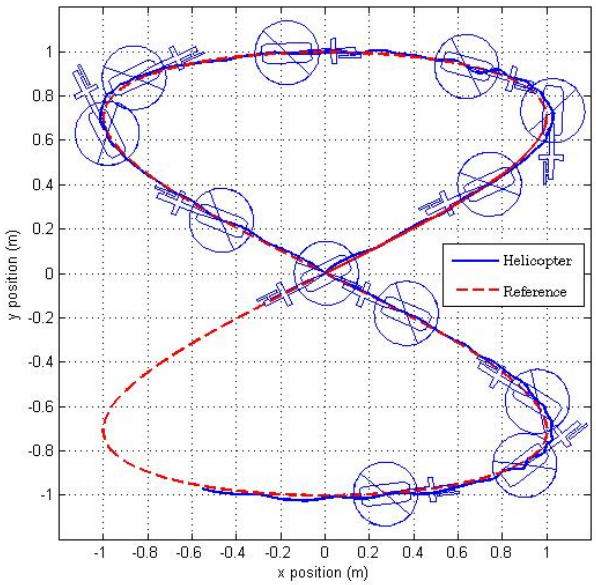

Figure 9: Eight-shape trajectory tracking

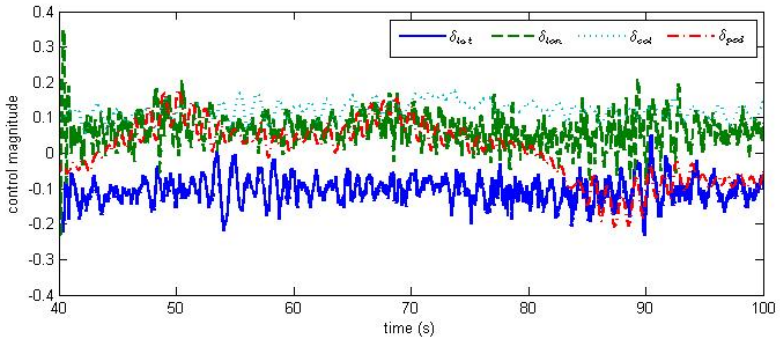

Figure 10: Control signals for eight-shape tracking

against the conventional MPC in the simulation and it demonstrates the excellent capability in the practical flight tests.

A Derivation of second derivative of position

By using the relationship in Eq.(21) the first three equations in the helicopter dynamics (4) can be simplified as follows

$$\begin{bmatrix} \dot{u} \\ \dot{v} \\ \dot{w} \end{bmatrix} = -\hat{\omega} \begin{bmatrix} u \\ w \\ w \end{bmatrix} + \mathbf{R}_i^b \begin{bmatrix} 0 \\ 0 \\ g \end{bmatrix} + \begin{bmatrix} 0 \\ 0 \\ T \end{bmatrix} \tag{47}$$

where $\mathbf{R}_i^b$ is a transformation matrix from inertial to body coordinates with the fact that $\mathbf{R}_i^b \mathbf{R}_b^i = \mathbf{I}_{3\times 3}$. On the other hand, differentiating (17) gives

$$\begin{bmatrix} \ddot{x} \\ \ddot{y} \\ \ddot{z} \end{bmatrix} = \mathbf{R}_b^i \hat{\omega} \begin{bmatrix} u \\ v \\ w \end{bmatrix} + \mathbf{R}_b^i \begin{bmatrix} \dot{u} \\ \dot{v} \\ \dot{w} \end{bmatrix} \tag{48}$$

By substituting Eq.(47) into Eq.(48) and cancelling the equivalent terms, one has the second derivative of position (19).

B Derivation of explicit MPC solution

By using the short notations of (43) and (44),we have the following relationship:

$$\bar{Y} - \bar{W} = \begin{bmatrix} M_\rho \\ M_1 \\ M_2 \\ \vdots \\ M_{r+1} \end{bmatrix} + \begin{bmatrix} 0_{(\rho_1+\cdots+\rho_4)\times 1} \\ A(\mathbf{x})\tilde{\mathbf{u}} \\ A(\mathbf{x})\tilde{\mathbf{u}}^{[1]} + p_1(\mathbf{x}, \tilde{\mathbf{u}}) \\ \vdots \\ A(\mathbf{x})\tilde{\mathbf{u}}^{[r]} + p_r(\mathbf{x}, \tilde{\mathbf{u}}, \cdots, \tilde{\mathbf{u}}^{[r-1]}) \end{bmatrix} = \begin{bmatrix} M_\rho \\ M_r \end{bmatrix} + \begin{bmatrix} 0 \\ H \end{bmatrix} \tag{49}$$

Hence, the performance index (33) can be further manipulated as

$$\begin{aligned} J =& \frac{1}{2}\left(\begin{bmatrix} M_\rho \\ M_r \end{bmatrix} + \begin{bmatrix} 0 \\ H \end{bmatrix} \right)^T \begin{bmatrix} \mathcal{T}_1 & \mathcal{T}_2 \\ \mathcal{T}_2^T & \mathcal{T}_3 \end{bmatrix} \left(\begin{bmatrix} M_\rho \\ M_r \end{bmatrix} + \begin{bmatrix} \mathbf{0} \\ H \end{bmatrix} \right) \\ =& \frac{1}{2} \begin{bmatrix} M_\rho \\ M_r \end{bmatrix}^T \begin{bmatrix} \mathcal{T}_1 & \mathcal{T}_2 \\ \mathcal{T}_2^T & \mathcal{T}_3 \end{bmatrix} \begin{bmatrix} M_\rho \\ M_r \end{bmatrix}^T + \frac{1}{2} \begin{bmatrix} M_\rho \\ M_r \end{bmatrix}^T \begin{bmatrix} \mathcal{T}_2 \\ \mathcal{T}_3 \end{bmatrix} H + \\ & \frac{1}{2} H^T \begin{bmatrix} \mathcal{T}_2^T & \mathcal{T}_3 \end{bmatrix} \begin{bmatrix} M_\rho \\ M_r \end{bmatrix} + \frac{1}{2} H^T \mathcal{T}_3 H \end{aligned} \tag{50}$$

It can be seen that the necessary optimal condition can be written as

$$\left(\frac{\partial H}{\partial \bar{\mathbf{u}}} \right)^T \begin{bmatrix} \mathcal{T}_2^T & \mathcal{T}_3 \end{bmatrix} \begin{bmatrix} M_\rho \\ M_r \end{bmatrix} + \left(\frac{\partial H}{\partial \bar{\mathbf{u}}} \right)^T \mathcal{T}_3 H = 0 \tag{51}$$

Recalling (49), the structure of $\frac{\partial H}{\partial \bar{\mathbf{u}}}$ is given in:

$$\frac{\partial H}{\partial \bar{\mathbf{u}}} = \begin{bmatrix} A(x) & 0_{4\times4} & 0_{4\times4} & \cdots & 0_{4\times4} \\ \times_{4\times4} & A(x) & 0_{4\times4} & \cdots & 0_{4\times4} \\ \vdots & \vdots & \vdots & \ddots & \vdots \\ \times_{4\times4} & \times_{4\times4} & \times_{4\times4} & \times_{4\times4} & A(x) \end{bmatrix} \tag{52}$$

where $\times_{4\times4}$ denotes the non-zero element. It can be seen that $\frac{\partial H}{\partial \bar{\mathbf{u}}}$ is invertible. Since $\mathcal{T}_3$ is positive definite, the necessary optimal condition implies:

$$H = -\begin{bmatrix} \mathcal{T}_3^{-1}\mathcal{T}_2^T & I_{(r+1)\times(r+1)} \end{bmatrix} \begin{bmatrix} M_\rho \\ M_r \end{bmatrix} \tag{53}$$

Extracting the first 4 equations from (53) yields the explicit solution to the MPC formulation (40).

References

[BW07] A. Bogdanov and E. Wan. State-dependent riccati equation control for small autonomous helicopters. *Journal of Guidance, Control, and Dynamics*, 30(1):47–60, 2007.

[CBG03] Wen-Hua Chen, Donald J. Ballance, and Peter J Gawthrop. Optimal control of nonlinear systems: a predictive control approach. *Automatica*, 39(4):633 – 641, 2003.

[GMF01] V. Gavrilets, B. Mettler, and E. Feron. Dynamic model for a miniature aerobatic helicopter. In *AIAA Guidance Navigation and Control Conference, Montreal, Canada*, 2001.

[HK09] J.K. Hedrick and Yeonsik Kang. Linear tracking for a fixed-wing uav using nonlinear model predictive control. *Control Systems Technology, IEEE Transactions on*, 17(5):1202–1210, Sept. 2009.

[Isi95] A. Isidori. *Nonlinear control systems*. Springer Verlag, 1995.

[JK05] E.N. Johnson and S.K. Kannan. Adaptive trajectory control for autonomous helicopters. *Journal of Guidance, Control, and Dynamics*, 28(3):524–538, 2005.

[KAM02] AS Krupadanam, AM Annaswamy, and RS Mangoubi. Multivariable adaptive control design with applications to autonomous helicopters. *Journal of Guidance, Control, and Dynamics*, 25(5):843–851, 2002.

[KB06] Tams Keviczky and Gary J. Balas. Receding horizon control of an f-16 aircraft: A comparative study. *Control Engineering Practice*, 14(9):1023 – 1033, 2006.

[KS98] T.J. Koo and S. Sastry. Output tracking control design of a helicopter model based on approximate linearization. In *Decision and Control, 1998. Proceedings of the 37th IEEE Conference on*, volume 4, pages 3635–3640, Dec 1998.

[KS03] H. Jin Kim and David H. Shim. A flight control system for aerial robots: algorithms and experiments. *Control Engineering Practice*, 11(12):1389 – 1400, 2003. Award winning applications-2002 IFAC World Congress.

[KSS02] H.J. Kim, D.H. Shim, and S. Sastry. Nonlinear model predictive tracking control for rotorcraft-based unmanned aerial vehicles. In *American Control Conference, 2002. Proceedings of the 2002*, volume 5, pages 3576–3581, 2002.

[LCA10] Cunjia Liu, Wen-Hua Chen, and John Andrews. Model predictive control for autonomous helicopters with computational delay. In *Control 2010, UKACC International Conference on*, Sept 2010.

[LCCAed] Cunjia Liu, Jonathan Clarke, Wen-Hua Chen, and John Andrews. Rapid prototyping flight test environment for autonomous unmanned aerial vehicles. *International Journal of Modelling, Identification and Control*, accepted.

[MN07] Lorenzo Marconi and Roberto Naldi. Robust full degree-of-freedom tracking control of a helicopter. *Automatica*, 43(11):1909 – 1920, 2007.

[MTK02] Bernard Mettler, Mark B. Tischler, and Takeo Kanade. System identification modeling of a small-scale unmanned rotorcraft for flight control design. *Journal of the American Helicopter Society*, 47(1):50–63, 2002.

[OM04] Anbal Ollero and Lus Merino. Control and perception techniques for aerial robotics. *Annual Reviews in Control*, 28(2):167 – 178, 2004.

[PCC+09] Kemao Peng, Guowei Cai, Ben M. Chen, Miaobo Dong, Kai Yew Lum, and Tong H. Lee. Design and implementation of an autonomous flight control law for a uav helicopter. *Automatica*, 45(10):2333 – 2338, 2009.

[SKC06] N. Slegers, J. Kyle, and M. Costello. Nonlinear model predictive control technique for unmanned air vehicles. *Journal of Guidance Control and Dynamics*, 29(5):1179–1188, 2006.

[SKS03] D.H. Shim, H.J. Kim, and S. Sastry. Decentralized nonlinear model predictive control of multiple flying robots. In *Decision and Control, 2003. Proceedings. 42nd IEEE Conference on*, volume 4, pages 3621–3626, Dec. 2003.